Chapter 17

Oblique Propagation

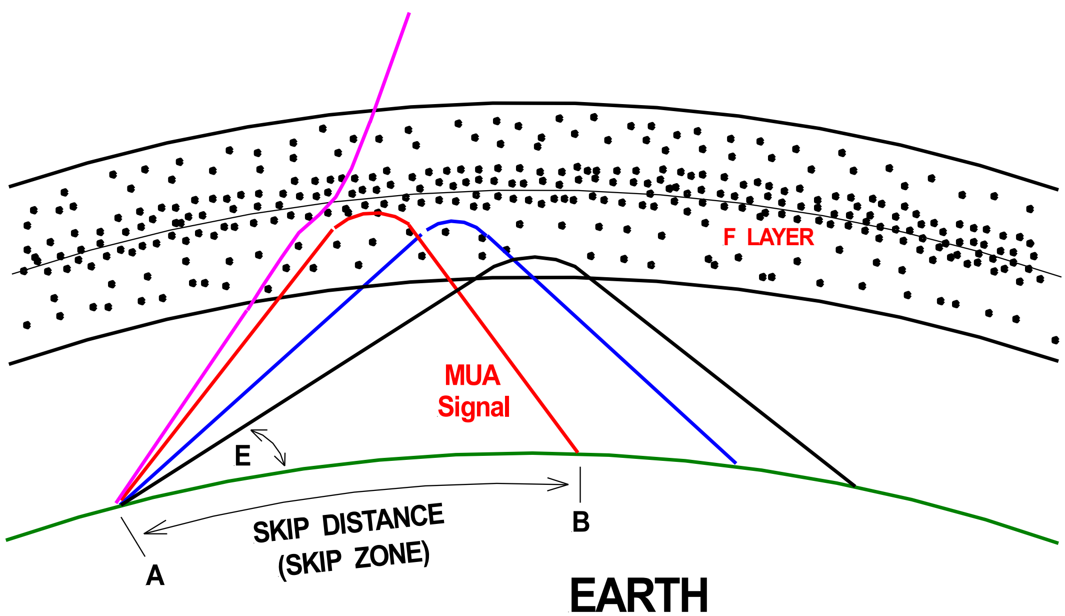

www.skywave-radio.org

17 Oblique Propagation

In the previous chapter we discussed NVIS communications distinguished by HF signals transmitted at high elevation angles over relatively short distances of 300 miles or less.

In this, and the following chapters, we discuss oblique propagation characterized by HF signals transmitted at relatively low angles over long distances ranging from 300 to many thousand miles.

Despite all of its attributes, oblique communication is often disrupted during the day by D Layer absorption. High angle NVIS signals (blue trace in Figure 1) pass through the D-Layer quickly incurring little absorption. However, low angle obliquely transmitted signals spend a significant amount of time traversing the D Layer, often resulting in the signals being completely absorbed as illustrated by the black trace in Figure 1. At night the D Layer disappears eliminating the absorption problem.

D-Layer absorption is inversely proportional to frequency squared, that is

$$\text{Absorption} \propto \frac{1}{f^2}$$

As a result, D Layer absorption on 40 meters is 1/4 that on 80 while on 20 meters it is only 1/16th of the 80 meter absorption. Consequently, D Layer absorption is a serious problem on 160 through 40 meters. But it is only a minor problem on 20 meters and negligible on 18 through 10 meters.

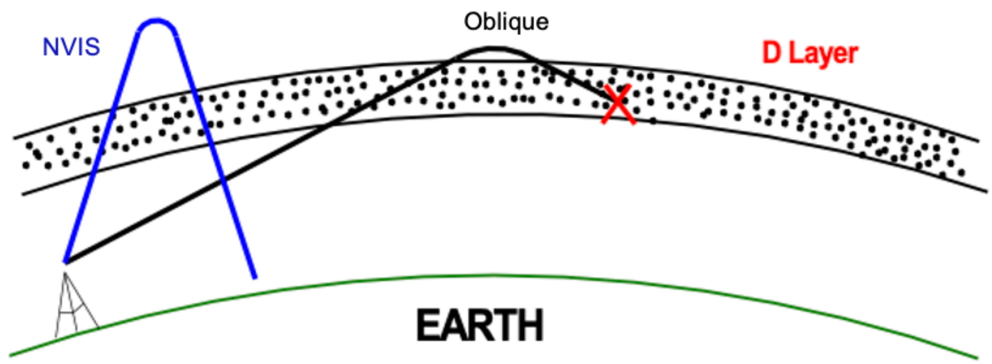

Figure 1 NVIS vs oblique D Layer absorption (source: author)

The transmitting frequency for NVIS communications must be below the ionosphere's critical frequency. However, oblique propagation can occur on frequencies both above and below the critical frequency. On 20 through 10 meters the transmitting frequency is always above the ionosphere's critical frequency and above the critical frequency most of the time on 30 meters. Consequently, NVIS is not possible at these frequencies. All HF communications on 30 through 10 meters is the result of oblique propagation. The transmitting frequency on 80 through 40 meters may be either above or below the critical frequency. Consequently, both NVIS and oblique propagation occur at various times on these frequency bands. 160 meters is always below the critical frequency.

80 and 160 meter oblique signals are absorbed during the day by the ionosphere's D Layer preventing daytime oblique communications on these bands. At solar maximum 80 meters is below the F Layer critical frequency all the time, as illustrated in Figure 2, permitting NVIS propagation during both day and night. The high angle of NVIS signals makes possible daytime NVIS communications even in the presence of D Layer absorption. At night 80 meter oblique communications is good in the absence of D Layer absorption. In the years of solar minimum (Figure 3), 80 meters is above the critical frequency at night providing good oblique communications but prohibiting NVIS propagation. 160 meters is nearly always below the critical frequency permitting good night time oblique communications.

Near solar maximum, 40 meters is below the daytime critical frequency. Because of its high elevation angle, 40 meter NVIS is excellent during the day, even in the presence of D Layer absorption. However, 40 meter oblique signals do not fare as well. During the day they are absorbed by the D Layer. The critical frequency drops below 40 meters at night prohibiting NVIS propagation. However oblique communication is good throughout the night. At solar minimum good 40 meter oblique propagation is available in the early evening as D Layer absorption disappears. But, late at night the critical frequency drops too low to support 40 meter oblique transmissions. 40 meter NVIS is not available at all during solar minimum.

These results are summarized in the Table 1.

The ionosphere's critical frequency is the upper frequency limit for NVIS. The frequency limit for oblique communications is the Maximum Usable Frequency (MUF). In Figure 4 the MUF is 20 meters. Frequencies higher than the maximum usable frequency penetrate the ionosphere and are lost to outer space as illustrated by the 15 meter signal in Figure 4. Signals transmitted at lower frequencies travel shorter distances. For example, a 40 meter signal (green trace in Figure 4) travels a shorter distance than the 20 meter MUF signal. An 80 meter signal travels even a shorter distance. The reason for this is that higher frequency signals travel higher into the ionosphere before being refracted back to Earth resulting in longer hops.

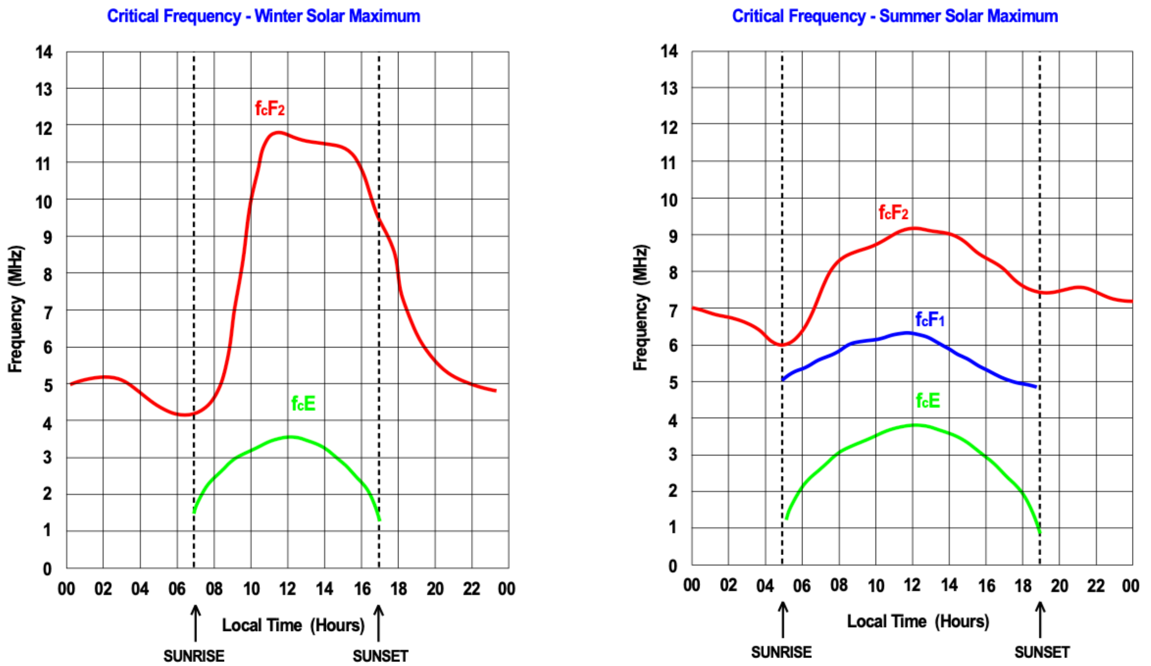

Figure 2 Winter and summer critical frequencies during solar maximum (source: author)

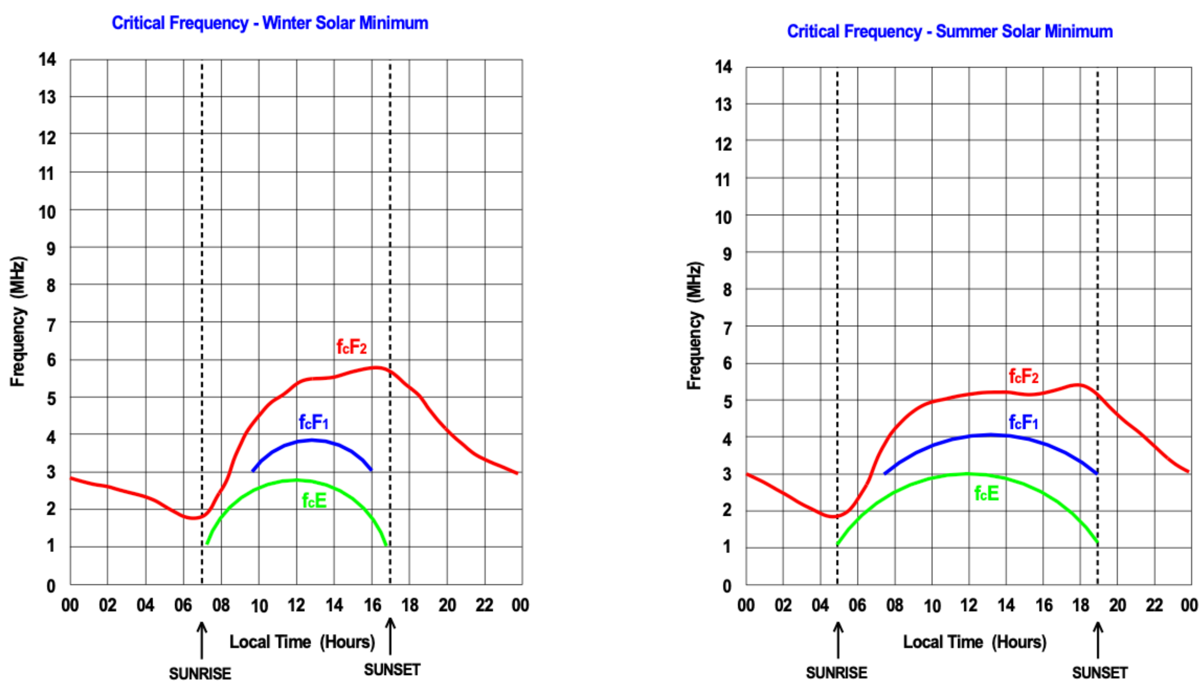

Figure 3 Winter and summer critical frequencies during solar minimum (source: author)

	Day	Evening	Night
80m Solar Max NVIS	Fair some absorption	Good $f_o < f_c$	Good $f_o < f_c$
40m Solar Max NVIS	Good $f_o < f_c$	Poor $f_o = f_c$	No NVIS $f_o > f_c$
80m Solar Min NVIS	Fair some absorption	Good $f_o < f_c$	No NVIS $f_o > f_c$
40m Solar Min NVIS	No NVIS $f_o > f_c$	No NVIS $f_o > f_c$	No NVIS $f_o > f_c$
80m Solar Max Oblique	Absorbed	Fair some absorb	Good
40m Solar Max Oblique	Absorbed	Good	Good
80m Solar Min Oblique	Absorbed	Absorbed	Good
40 m Solar Min Oblique	Fair some absorption	Good	None f_c too low
160m Solar Max & Min	Absorbed	Absorbed	Good

Table 1 Propagation Conditions (source: author)

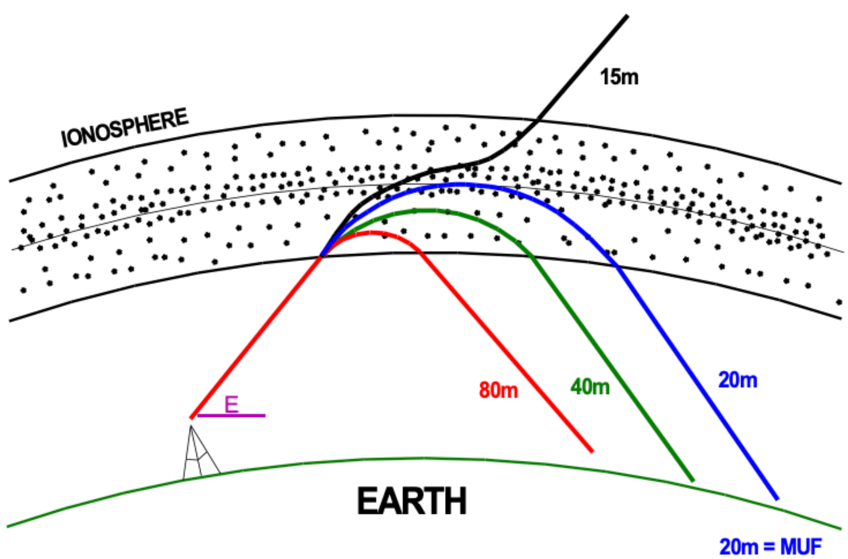

Figure 4 Hop distance verses operating frequency (source: author)

Maximum usable frequency is determined by the ionosphere's critical frequency f_c and the elevation angle E at which a signal is transmitted. The angle E varies from 0 degrees, horizontal to the ground, to 90 degrees straight up. The equation for maximum usable frequency is

$$MUF = \frac{f_c}{\sin E}$$

The "sin E" term is equal to zero at an elevation angle of 0^o and equal to one at 90^o. Since "sin E" ranges between 0 and 1, MUF is always equal to or greater than the critical frequency.

As usual, the current critical frequency is obtained by clicking on Critical Frequency under the Current Conditions tab of the www.skywave-radio.org website. A typical critical frequency map is shown in Figure 5. This particular map shows the critical frequency for September 28, 2025 at 17:30 UT (10:30 Pacific Daylight Time). Over California the critical frequency was 11 MHz.

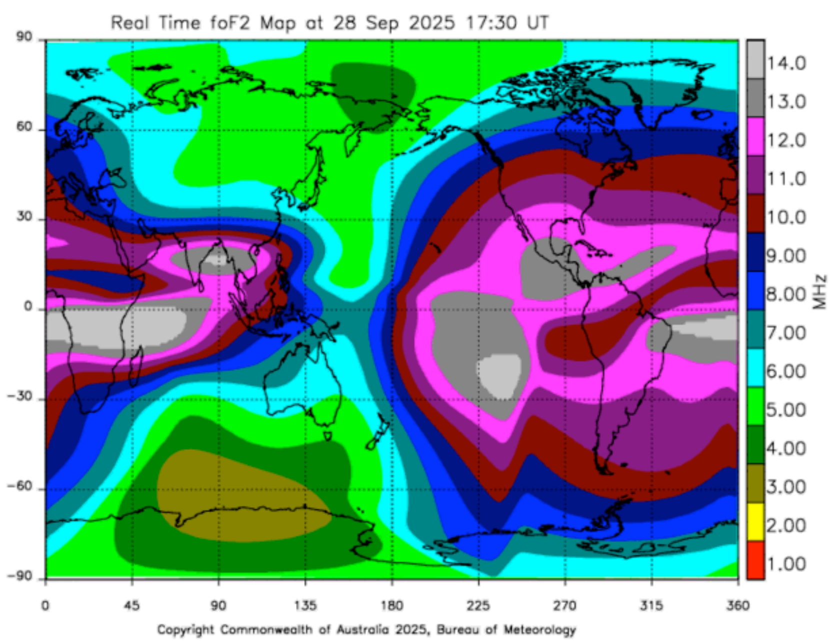

Figure 5 Critical frequency map for September 28, 2025 at 17:30 UT (10:30 PDT)

The distance traveled by a signal depends on its elevation angle E in addition to its frequency. The lowest angle signal in Figure 6 (the black trace) travels the furthest. The distance traveled decreases as the elevation angle increases. The highest angle at which a signal can be transmitted and return to Earth is called the Maximum Usable Angle (MUA). Transmitting at an angle greater than the MUA causes the signal to penetrate the ionosphere and be lost to space, for example the magenta trace in Figure 6. The maximum usable angle depends on the critical frequency f_c and the frequency of the signal being transmitted f_o according to the following equation.

$$MUA = E_M = \sin^{-1}\left[\frac{f_c}{f_o}\right]$$

Note that a signal will penetrate the ionosphere and be lost to outer space if its frequency is greater than the maximum usable frequency (MUF) or it is transmitted at an angle greater than the maximum usable angle (MUA).

The shortest distance that can be covered by an obliquely transmitted signal occurs at an elevation angle equal to the MUA illustrated by point B in Figure 6. To reach a closer station the transmitter at point A would have to transmit at an angle greater than the MUA which would of course cause the signal to penetrate the ionosphere and be lost. Thus, the region from point A to point B is a skip zone. The radio station at point A can not transmit to or hear any stations in the skip zone. These stations are ”skipped over”.

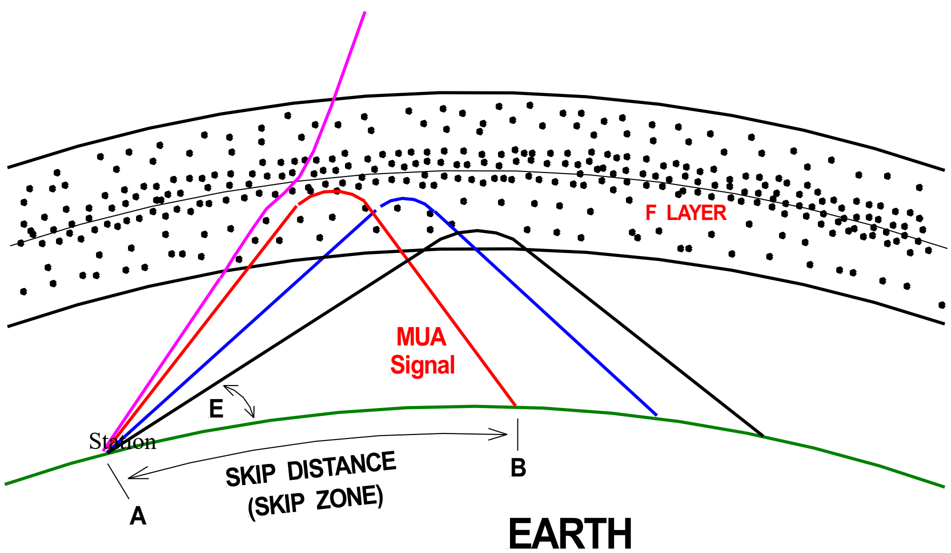

Figure 6 Skip distance and associated skip zone (source: author)

It is important to note in Figure 7 that a skip zone always exists for oblique transmissions at frequencies above the critical frequency. But transmissions at frequencies below the critical frequency, including both oblique and NVIS, do not have a skip zone. Thus, a skip zone is always present when operating on 20 through 10 meters. A skip zone may or may not be present on 80 through 30 meters, depending on conditions.

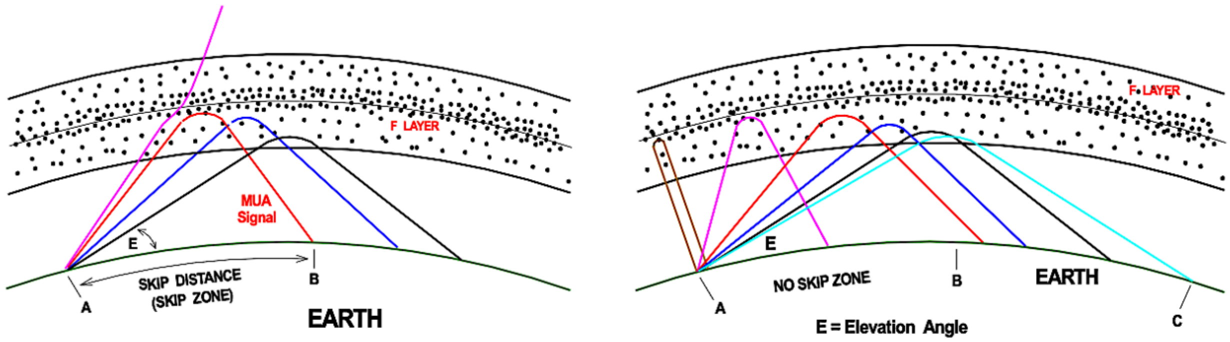

Oblique Propagation Skip Zone when $f_o > f_c$ No Skip Zone when $f_o < f_c$

Figure 7 Oblique and NVIS Propagation (source: author)

The various forms of oblique propagation include:

- F mode propagation,
- E mode propagation,
- Sporadic E propagation,
- Multi-path propagation,
- Backscatter,
- Great Circle propagation,
- Gray Line propagation,
- Equatorial Sporadic E propagation,
- Transequatorial Propagation (TEP), and
- Ionospheric Ducting

17.1 F Mode Propagation

Long distance HF communications results from one or more hops through the F region of the ionosphere. As illustrated in Figure 8, a long distance signal:

- Passes through the ionosphere's D and E layers,

- Refracts in the F region of the ionosphere,

- Travels again through the E and D layers on its way back to Earth, and

- Reflects from the Earth's surface beginning another hop.

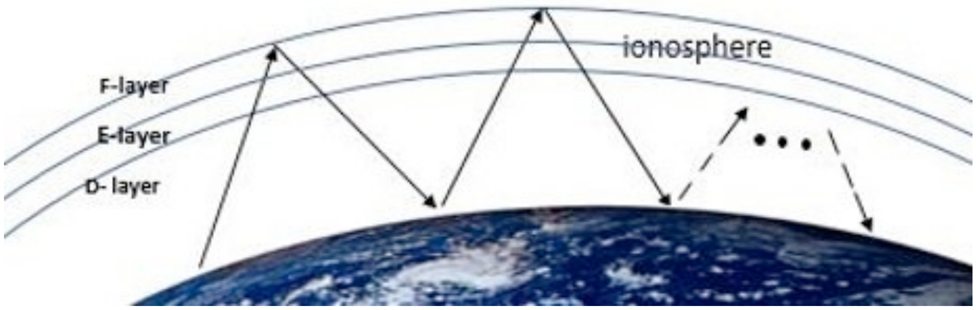

Figure 8 Multiple hop propagation through the ionosphere (source: ResearchGate)

With each hop the strength of the transmitted signal decreases limiting the distance that a radio signal can travel. Losses are primarily due to:

- Energy absorbed in each pass of the signal through the D Layer, and
- Ground losses with each reflection from the Earth's surface

As described above, D Layer absorption is inversely proportional to frequency squared

$$\text{Absorption} \propto \frac{1}{f^2}$$

As a result, D Layer absorption on 40 meters is 1/4 that on 80 while on 20 meters it is only 1/16th of the 80 meter absorption. To minimize D-Layer absorption, operate on the highest available frequency during the day. Absorption is not a problem at night when the D Layer disappears. Consequently, communications over longer distances are possible at night.

Reflections from the ocean's surface are typically attenuated 0.5 db while a signal reflecting from poorly conducting arid soil can be attenuated 3 db or more.

Absorption in the D region coupled with ground losses limit most long distance oblique communications to 3 or 4 hops. Under ideal conditions, 5 to 6 hops may be possible particularly over the ocean. Usually, however, more than 4 hops result in signals which are too weak to be received. Consequently, long distance communication depends on each hop being as long as possible, enhanced by using high transmitting power and high gain directional antennas.

The distance traveled on each hop depends on:

- The operating frequency: signals transmitted at the maximum usable frequency (MUF) travel the furthest,
- The ionosphere's critical frequency: a high critical frequency increases the maximum usable frequency and thus hop distance,
- The elevation angle at which signals are transmitted: low angles result in long hops,
- Height of the ionosphere's F2 region: longer hops are achieved with a high F2 region.

The characteristics of the transmitting antenna determine the lowest angle at which a signal can be transmitted. The radiation pattern for a typical 20 meter Inverted-V antenna 1/2 wavelength above ground is shown in Figure 9. In this figure the lowest angle at which this antenna can effectively radiate a signal is approximately 10^o. This is the antenna's Lowest Radiated Angle or LRA. LRA is defined as the angle at which the antenna's radiated power is 6 db below its maximum level. The power radiated by an antenna drops off very quickly below its LRA with nearly all of the antenna's energy radiated at higher angles. For example, the power radiated by this antenna at an elevation angle of 15^o is 3 db higher, twice that radiated at its LRA. Similarly, Highest Radiated Angle (HRA) is the upper angle at which the antenna's radiated power is 6 db below its maximum level.

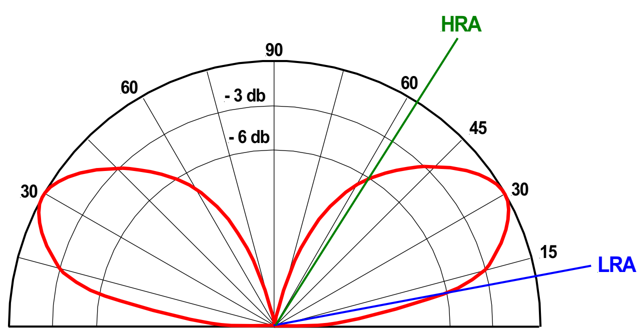

Figure 9 Radiation pattern for a typical 20 meter Inverted-V antenna (source: author)

An antenna's LRA along with the height of the ionosphere's F region directly affects the maximum hop distance that the antenna can achieve, as shown in Figure 10. At a F2 height of 350 km the hop distance is approximately 1250 miles for a signal transmitted at an elevation angle of 15^o. The current height of the ionosphere is found by clicking on Vertical Soundings under the Current Conditions tab of the www.skywave-radio.org website and following the provided instructions.

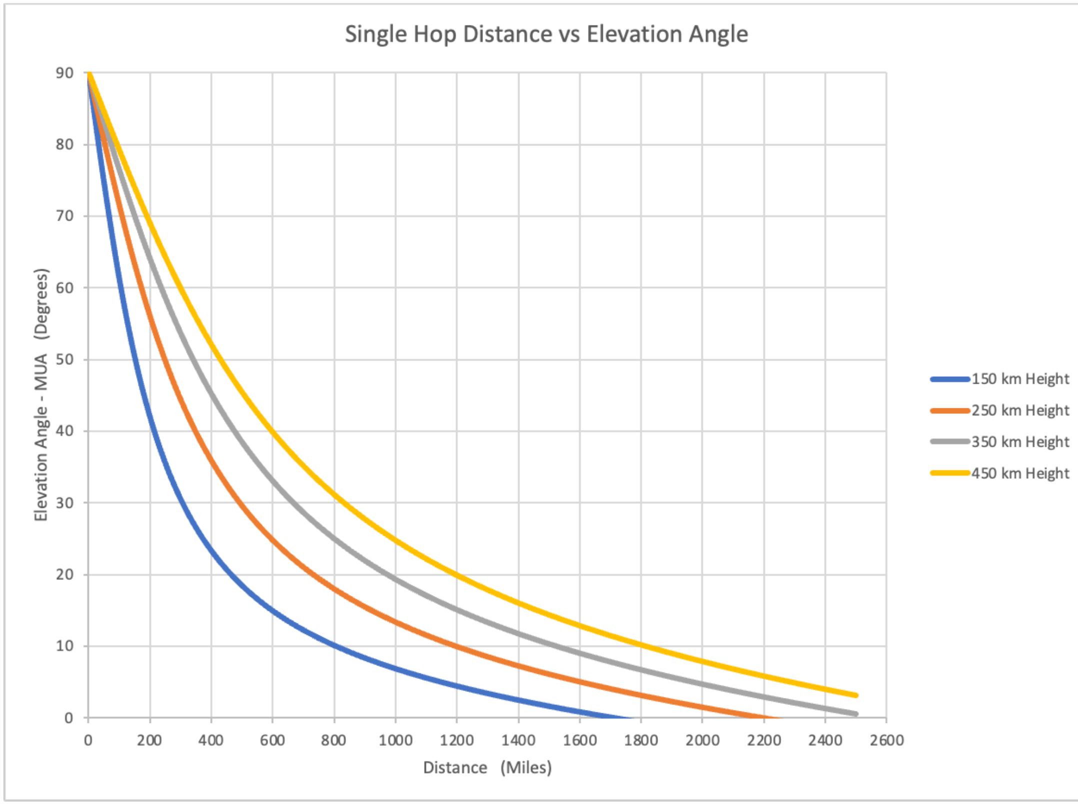

Figure 10 Hop distance verses elevation angle (source: author)

17.2 E Mode Propagation

Radio waves refract back to Earth from both the ionosphere's E and F regions as illustrated in Figure 11. Because of its lower height, hops through the E region are shorter than those through the F layer requiring more hops to reach a particular destination. This means more passes through the signal absorbing D region and more ground reflection losses. Consequently, E mode propagation generally results in received signal strengths being less than those through the F region.

A transmitted signal will bend back to Earth in the ionosphere's E region if the signal's elevation angle is below the E region Maximum Usable Angle (MUA_E).

$$MUA_E = \sin^{-1}\left[\frac{f_{cE}}{f_o}\right]$$

where f_{cE} is the E region critical frequency and f_o is the operating frequency. When this occurs the E region acts like a shield preventing low angle signals from reaching the F region. As a result, the hop distances for low angle signals are dramatically shortened compared to their normal long hops through the F layer.

E region shielding adversely affects long distance (DX) communications. This typically occurs around noon time when the E region critical frequency is the highest. The E region's noon time critical frequency f_{cE} during solar maximum is 3 to 4 MHz. During solar minimum the noon time critical frequency is 2 to 3 MHz as shown in Figure 12.

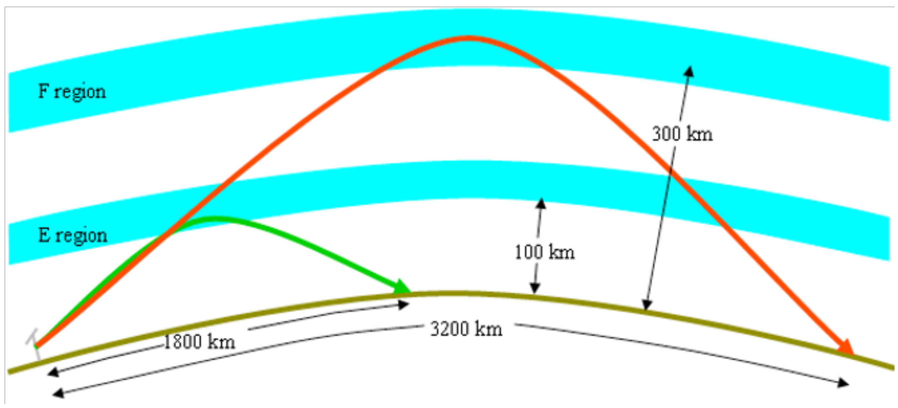

Figure 11 E and F mode propagation (source: Space Weather Service)

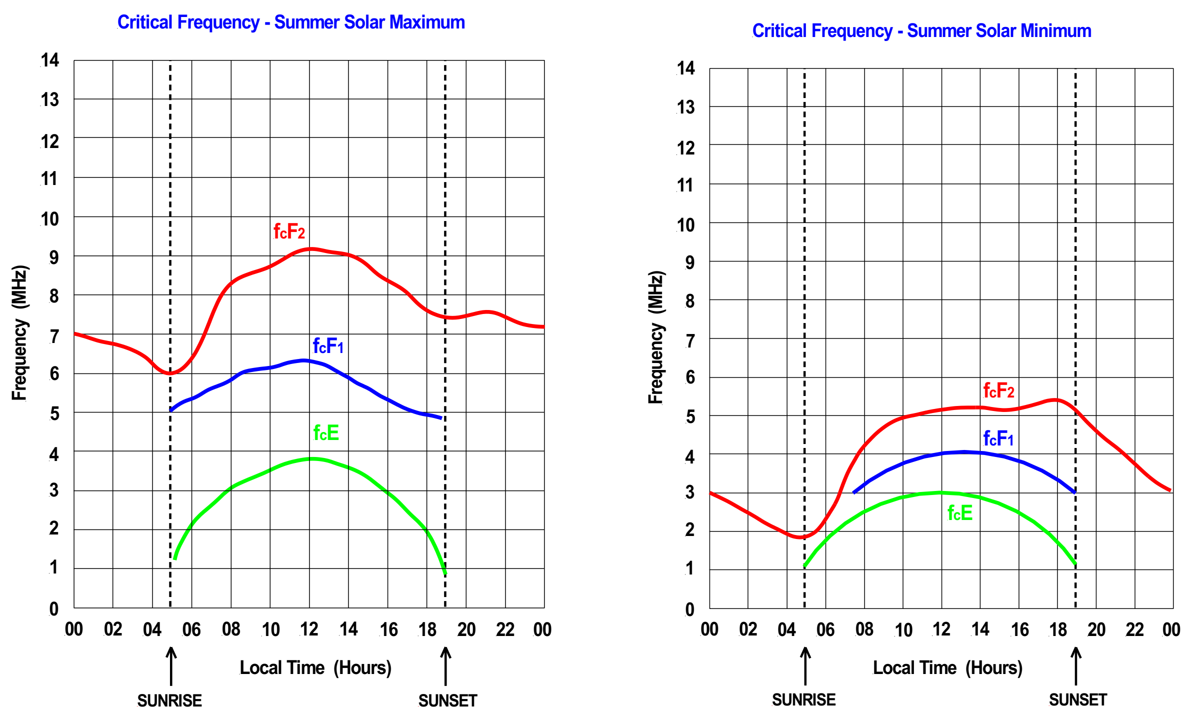

Figure 12 Critical frequencies during solar maximum and minimum (source: author)

40 meter hop distance increases as the elevation angle of the transmitted signal drops. At an elevation angle of 10° the hop distance is 1,400 miles, as illustrated in Figure 13. However, the E region mid-day critical frequency (fcE) is 3 to 4 MHz resulting in a E region maximum usable angle of 29°. This causes 40 meter signals transmitted at angles below 29° to refract in the E region instead of reaching the F2 layer. For completeness:

$$MUA_E = \sin^{-1}\left[\frac{f_{cE}}{f_o}\right] = \sin^{-1}\left[\frac{3.5\ MHz}{7.1\ MHz}\right] = \sin^{-1}[0.49] = 29°$$

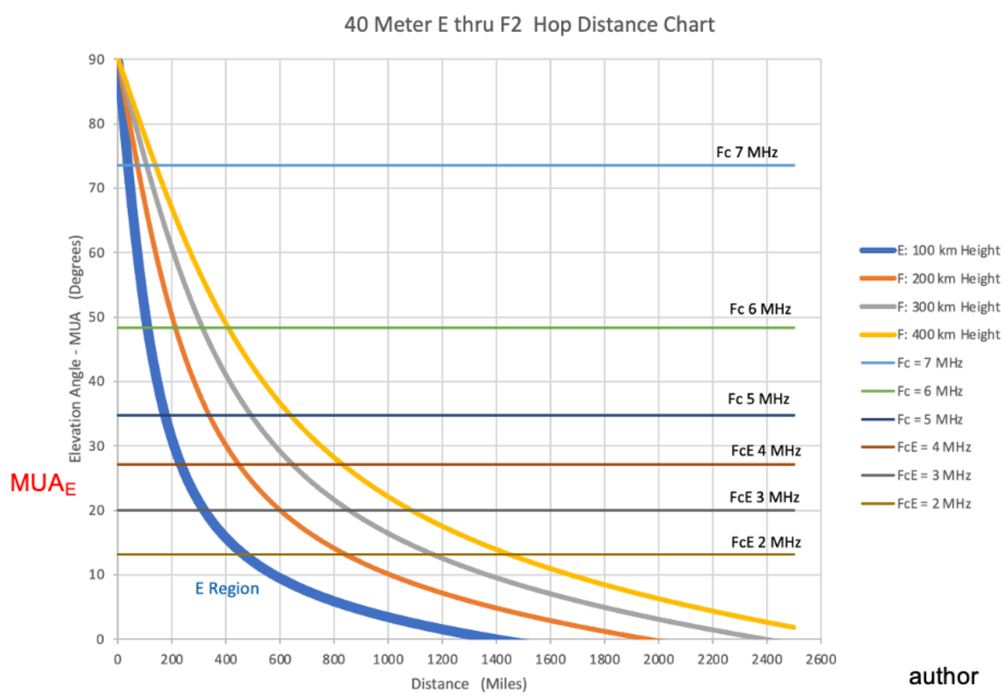

Figure 13 40 meter hop distances E through F2 regions

The effect of E region screening is illustrated in Figure 13. At an F region height of 300 km (gray trace) the hop distance for a 40 meter signal transmitted at an angle of 30° is about 600 miles. At elevation angles of 29° and below, E mode propagation occurs represented by the thick blue trace in Figure 13. At 29° hop distance suddenly drops from the F2 distance of 600 miles to the E mode hop distance of only 200 miles. In essence, long distance communications through the ionosphere's F region stops at elevation angles equal to and below MUA_E. E region screening has a more detrimental effect on 40, 30, and 20 meter mid-day DX than D layer absorption. D layer absorption is often blamed for poor mid-day DX while E region screening is often the culprit.

17.3 Sporadic E Propagation

Sporadic E (E_s) formations of abnormally high ionization within the E region (Figure 14) are important because they can reflect HF radio signals at frequencies up to about 100 MHz. They are called sporadic E because they randomly appear in various sizes and shapes, persist for minutes to hours, and occur from one day to the next with little predictability. Sporadic E zones are relatively large structures about 2 kilometers thick with horizontal dimensions stretching hundreds of kilometers. In general, sporadic E appearances seem to have little direct relationship to the ionization processes responsible for the E region itself.

Sporadic E zones often have electron densities far greater than normal E region levels and at times even greater than in the F region. Sporadic E patches can appear opaque to radio waves, reflecting waves that normally would have been refracted high in the F2 layer. This can seriously impact HF radio circuits. Instead of a single hop through the ionosphere, multiple hops with more ground reflections and more passes through the attenuating D region may be required to reach a destination. This is illustrated on the left in Figure 15. This can seriously degrade signal levels at the receiving site. Worse yet, the intended receiving location could be missed altogether as occurs on the right in Figure 15. At times sporadic E patches are partially transparent or patchy permitting radio waves to penetrate through the gaps. However, a partially transparent sporadic E patch often leads to weak or fading signals as the sporadic E zone evolves.

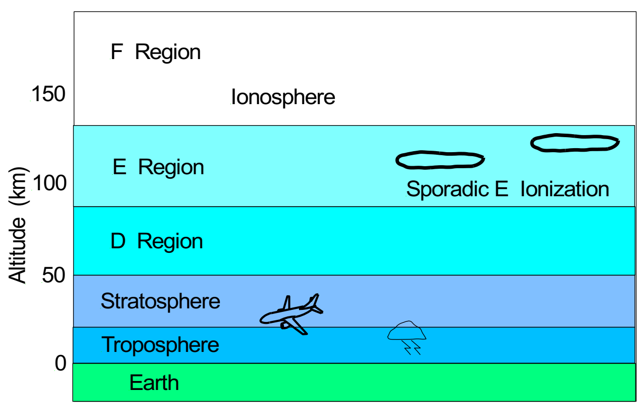

Figure 14 Sporadic E ionization (source: author)

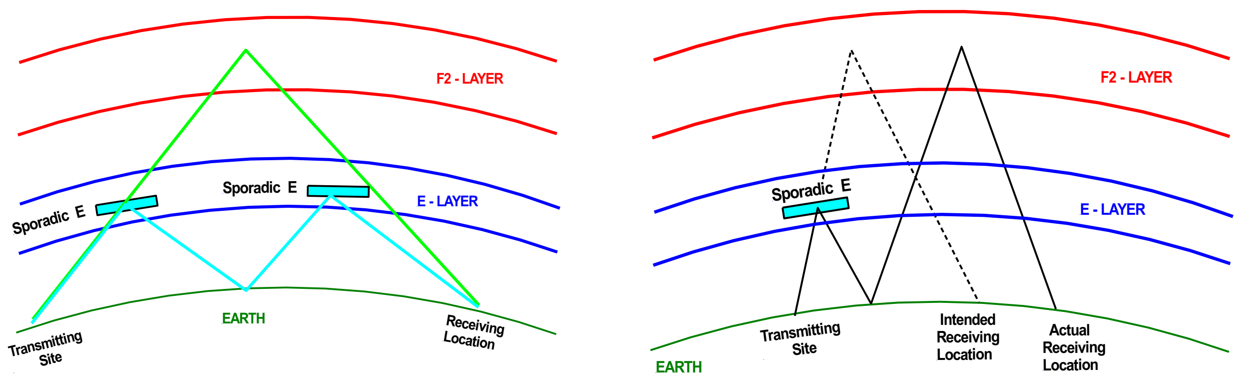

Figure 15 Disruptions in propagations paths due to sporadic E (source: author)

Figure 16 illustrates the important fact that sporadic E reflections can occur on the top side of the E region as well as on the bottom side shown in Figure 15.

Sporadic E zones are particularly strong in the low latitude equatorial region where they are essentially a daytime phenomenon with little seasonal variation. It is believed that they are formed in this part of the world by instabilities in the equatorial electrojet illustrated in Figure 17.

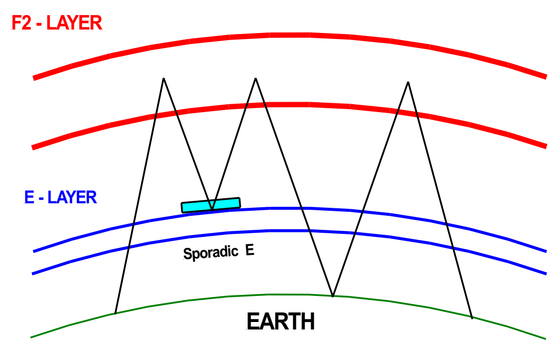

Figure 16 Topside Sporadic E reflection (source: author)

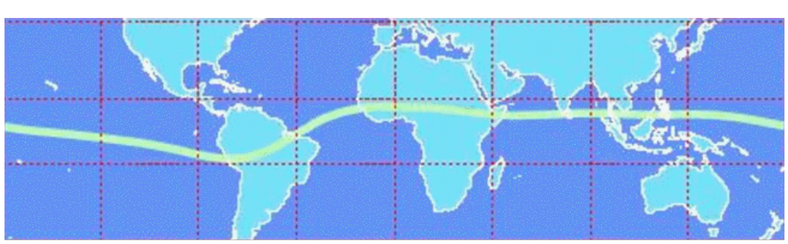

Figure 17 Equatorial electrojet (source: gfz-potsdam.de)

At mid latitudes sporadic E zones tend to be weaker than elsewhere. Their occurrence is subject to diurnal and seasonal variations. They tend to be more prevalent during the summer than in winter and during the day than at night, occurring often in mid-morning and near sunset. It is believed that sporadic E patches at mid latitudes form as the result of wind shear in the upper atmosphere in combination with meteoric debris. Enormous numbers of meteors burn up in the E region of the atmosphere (Figure 18). The meteoric debris is largely monatomic metallic ions consisting of iron, sodium, magnesium, and other similar elements. These monatomic ions are relatively small compared to the much larger molecular ions which comprise the E region. Because of their small size, the rate of electron-ion recombination is lower than for molecular ions.

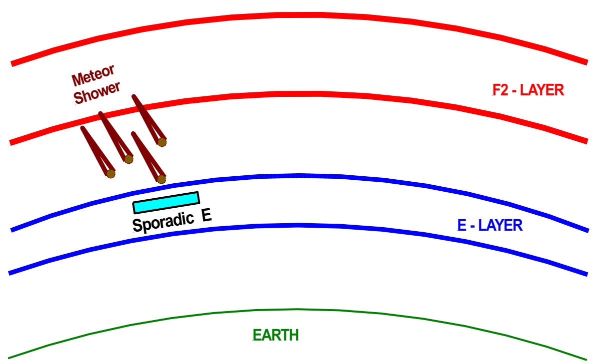

Figure 18 Meteor showers creating sporadic E patches (source: author)

Atmospheric gravity waves, associated with traveling ionospheric disturbances (TIDs), create upper atmosphere high velocity winds that travel in opposite directions at slightly different altitudes (Figure 19). This set of conditions produce what is known as vertical wind shear. Meteoric debris becomes trapped between the wind reversals at locations where the wind velocity tends to be low. Within the pockets of trapped debris, the rate of electron-ion recombination (the rate of electron loss) is lower than elsewhere in the E region. Consequently, relatively high electron concentrations develop in these pockets producing sporadic E patches.

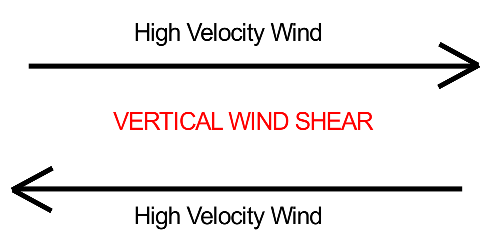

Figure 19 Vertical wind shear (source: author)

At high latitudes sporadic E zones occur mainly at night with little seasonal variance. They are attributed to ionization by incoming high energy charged particles entering the auroral region from the magnetosphere. Clouds of auroral E_s drift westward in the evening and eastward in the early morning at speeds between 200 and 3,000 meters per second, much like the auroral itself. Sporadic E zones within the polar caps have a different characteristic. They are weaker and extend across the polar caps in the form of ribbons in a roughly sunward direction.

17.4 Multi-path Propagation

Communications between Los Angeles and Denver, a distance of 800 miles, can occur on 40 meters in either one hop or in two hops of 400 miles each as illustrated in Figure 20.

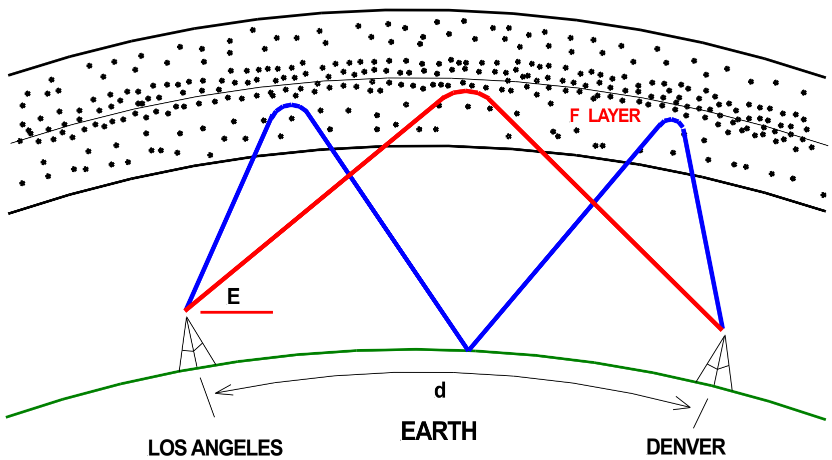

Figure 20 Communications between Los Angeles and Denver (source: author)

The 40-meter skip distance chart in Figure 21 shows that at a F2 region height of 350 km (gray trace) an elevation angle of roughly 25° is needed to reach Denver in one hop while an angle of 45° is required for the double hop path. A critical frequency of 6.0 MHz and greater supports both paths. Note that skip distance charts are available under the Tools tab of the www.skywave-radio.org website.

In general, we have relatively little control over the elevation angle at which our antenna radiates. The 40-meter half wavelength dipole (solid trace in Figure 22) radiates well at all angles from 15 to 60°. Radiation from this antenna will reach Denver following both the single and double hop propagation paths. There is nothing that we can do about that!

The single and double hop signals will be out of phase when they arrive in Denver since the double hop signal has to travel a longer distance to reach Denver. Consequently, the two signals will interfere with each other reducing the strength of the received signal, in addition to producing distortion and fading.

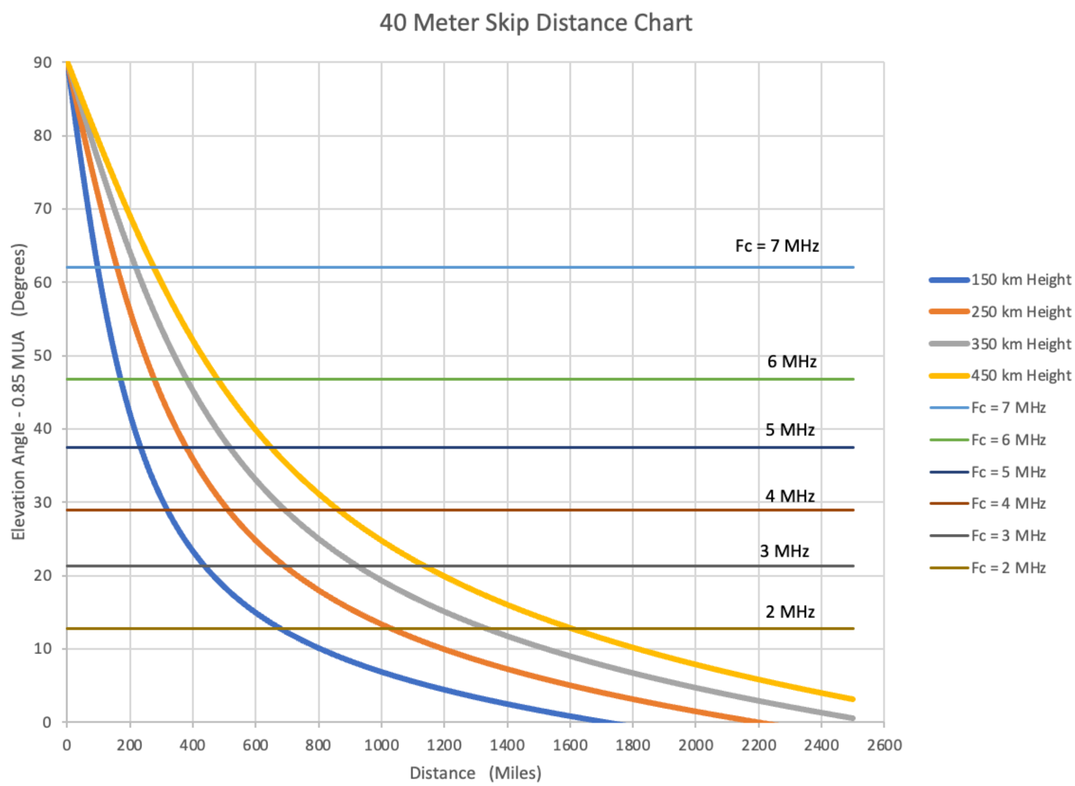

Figure 21 Skip distance chart - 40 meters. (source: author)

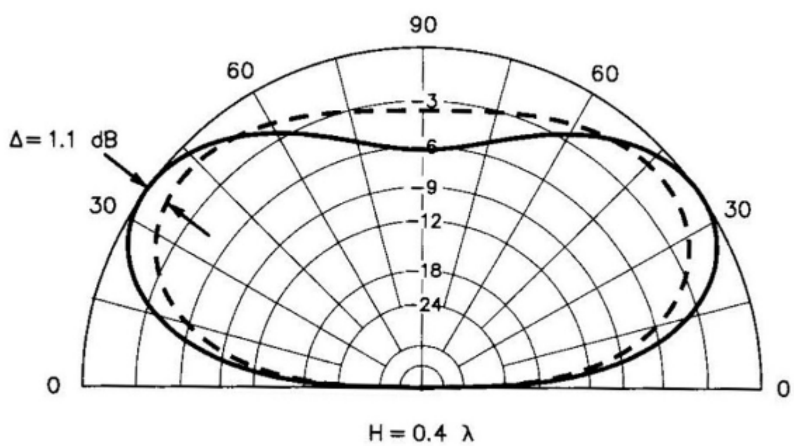

Solid Trace = Dipole Dashed Trace = Inverted V

Figure 22 Elevation pattern for a 40 meter horizontal antenna (source: ON4UN Low-Band DXing)

The MUF at a critical frequency of 6.0 MHz and an elevation angle of 25° is

$$[MUF]_{25^\circ} = \frac{f_{cF2}}{\sin E} = \frac{6.0\ MHz}{\sin 25} = 14.2\ MHz$$

At an elevation angle of 45° the maximum usable frequency is

$$[MUF]_{45^\circ} = \frac{f_{cF2}}{\sin E} = \frac{6.0\ MHz}{\sin 45} = 8.5\ MHz$$

Consequently, the double and single hop propagation modes are supported since the 40-meter operating frequency of 7.2 MHz is below the MUF for both the 25° and 45° elevation angles.

The 25° elevation angle MUF of 14.2 MHz allows communications with Denver on 30 meters (10.1 MHz), but the 45° elevation angle (MUF = 8.5 MHz) does not. This is illustrated by the 30-meter skip distance chart in Figure 23. In this chart an elevation angle of 45° is above the 31° angle permitted by the 6.0 MHz critical frequency. Transmitting at an elevation angle of 45° on 30 meters will result in the transmitted signal being lost to outer space. However, Denver is easily reached by transmitting on 30 meters at an elevation angle of 25°. In fact, this is the only possible path to Denver on 30 meters. Moving from 40 to the 30 meter frequency band eliminates the Los Angeles to Denver multi-path interference problem.

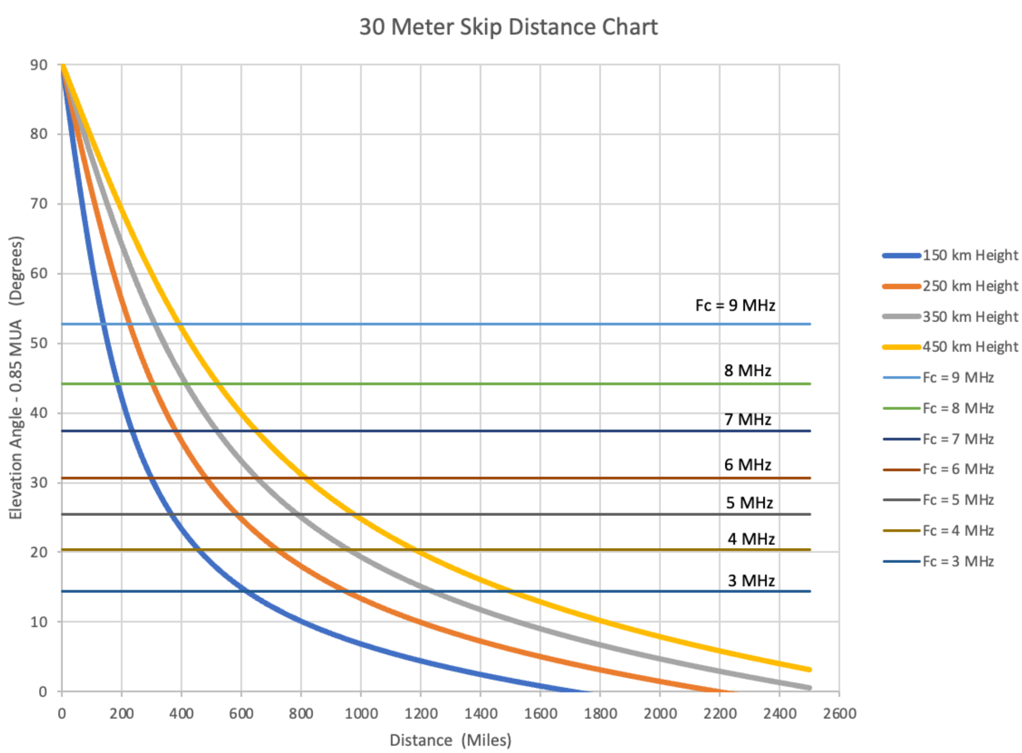

Figure 23 Skip distance chart - 30 meters (source: author)

This brings us back to a common theme. Optimum communications through the ionosphere is achieved by operating at the highest possible frequency.

17.5 Ground Scattering of Radio Waves and Backscatter

We assume in our simple Figure 24 propagation diagram that our radio waves reflect back and forth between the ionosphere and a smooth flat Earth in route to the receiving station. This over simplification is usually not the case.

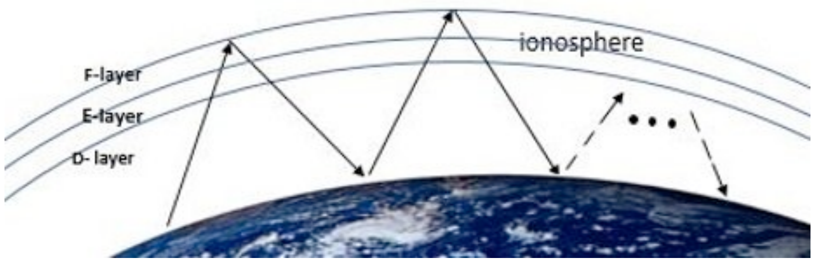

Figure 24 Multiple hop propagation through the ionosphere (source: ResearchGate)

Our assumption of a smooth flat Earth is analogous in many ways to scenery perfectly reflecting from the surface of the very smooth lake shown in Figure 25. In terms of reflection, the average depth of surface irregularities must be substantially less than the wavelength of the incident light, or radio wave, to be a perfectly smooth surface. Radio waves do at times perfectly reflect from a smooth flat Earth according to our simplistic propagation model. But again, this is usually not the situation.

Figure 25 Reflections from a perfectly smooth lake. (source: Wikipedia)

If the surface of a lake is not perfectly smooth, reflected light will be scattered in all directions producing the blurry image shown in Figure 26. The same is true of radio waves. The depth of surface irregularities in hilly terrane is considerably larger than the wavelength of incident radio waves, scattering the radio waves in multiple directions. Some of the scattered radio waves will be reflected in the desired propagation direction. Radio waves scattered in other directions will be lost resulting in ground scatter attenuation.

Figure 26 Blurry reflections from a rough lake (source: olympus-lifescience.com)

Some of the scattered signal may travel back through the ionosphere toward the transmitting site as illustrated by the blue trace in Figure 27. This is known as backscatter. Often backscattered signals end up in the skip zone. When this occurs, a few of the stations in the skip zone may hear the transmitting station when normally they would not.

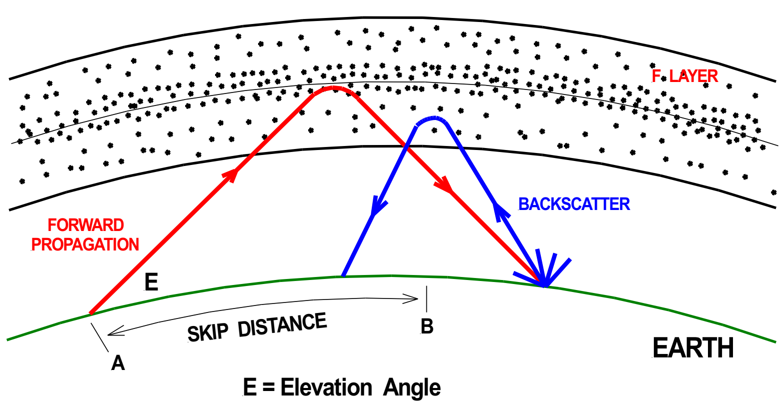

Figure 27 Backscatter propagation (source: author)

17.6 Great Circle Propagation

A great circle path is the shortest distance between any two locations on Earth's surface. A great circle is formed by a plane passing through the two points of interest and the center of the Earth as shown in Figure 28. A great circle always divides the Earth in half. Thus, the equator and lines of longitude are great circles. However, lines of latitude are not great circles since they do not cut the Earth in equal halves.

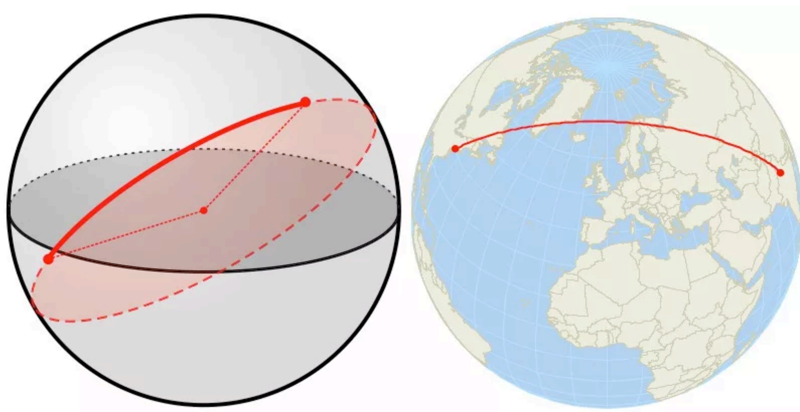

Figure 28 Great Circle path (source: Caliper Corporation)

Normally, radio waves follow great circle paths since a great circle is the shortest distance between the transmitting and receiving stations. However, high latitude ionospheric irregularities including

- Ionospheric tilt
- Troughs,
- High latitude spread F,
- Patches,
- Blobs, and
- Traveling Ionospheric Disturbances,

can seriously alter signal propagation paths. For example, a signal intended to travel along the great circle path over the polar region from eastern United States to India (Figure 28) could instead end up in Egypt or perhaps Korea. In general, great circle paths become less meaningful for signals propagating through Earth's polar zones.

17.7 Gray Line Propagation

In Figure 29 the line dividing night and day is called the terminator. It is also referred to as the gray line and twilight zone. It is actually a fuzzy line due to the bending of sunlight in Earth's atmosphere. Thus, a more appropriate term would be gray zone.

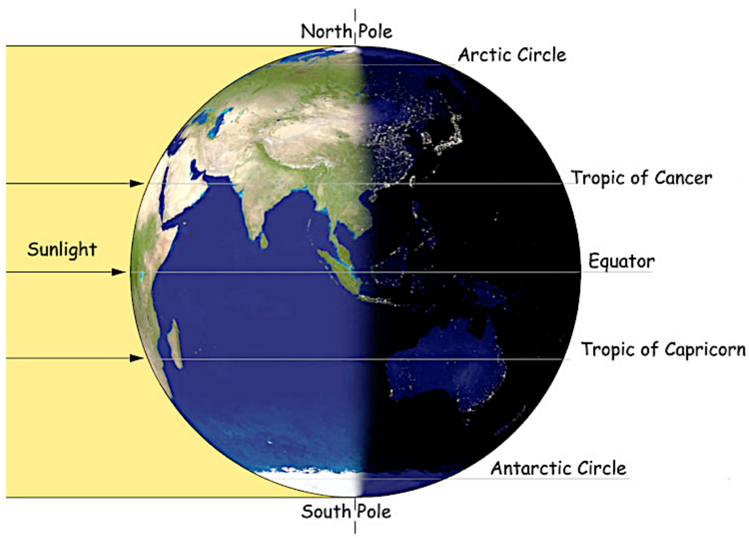

Figure 29 Earth's terminator (source: cseligman.com)

The position of the gray line is constantly changing as the Earth rotates throughout the day and orbits around the Sun during the year. As illustrated in Figure 30, the Earth's axis is always tilted 23.5^{o} with respect to its orbit. In Figure 30, the gray line runs north and south passing through the Earth's geographic poles during the March 21 and September 21 solar equinoxes. During the December and June solstices (December 21 and June 21), the gray line is tilted 23.5^{o} with respect to Earth's axis, as shown in Figures 30. During the course of a year, the gray line traverses a 47^{o} sector of the Earth north and south of the equator as the Earth orbits the Sun. The width of the gray zone also varies. The transition between night and day occurs quickly near the equator while in the polar zones it occurs more slowly. Consequently, the gray zone is wider at high latitudes than at the equator.

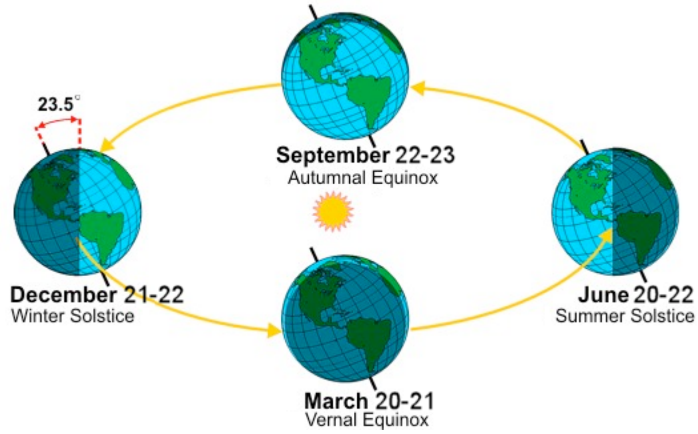

Figure 30 Earth's orbit around the Sun (source: NOAA National Weather Service)

The ionosphere changes significantly during sunrise and sunset. At sunrise the F region builds rapidly as solar ionization resumes. The D layer also reappears but more slowly. The reverse occurs in the evening. The D layer disappears soon after sunset while the F region slowly decays throughout the night. The delay between the appearance and disappearance of the D region relative to the F layer, illustrated in Figure 31, provides a period of enhanced communications.

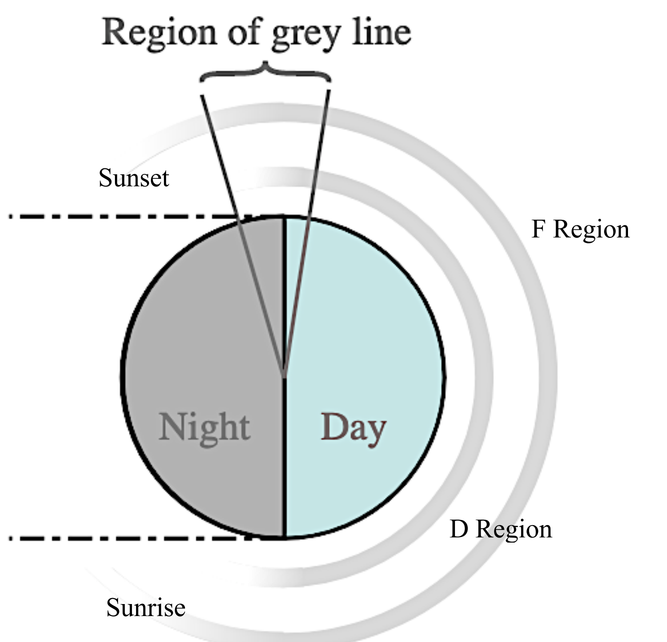

Figure 31 Gray line formation (source: Electronics Notes)

In the morning a strong F region permits excellent communications along the gray line before the signal absorbing D layer has a chance to develop. In the evening the D layer disappears quickly again permitting a period of excellent communications while the F region is still strongly ionized.

In Figure 32 excellent communications from northern Europe to eastern Africa occurs at sunrise. In western Canada good communications into the south Pacific occurs at sunset. Seasonal variations in gray line orientation provide optimum paths to slightly different parts of the world each day. These periods of enhanced communications last for about 45 minutes to an hour.

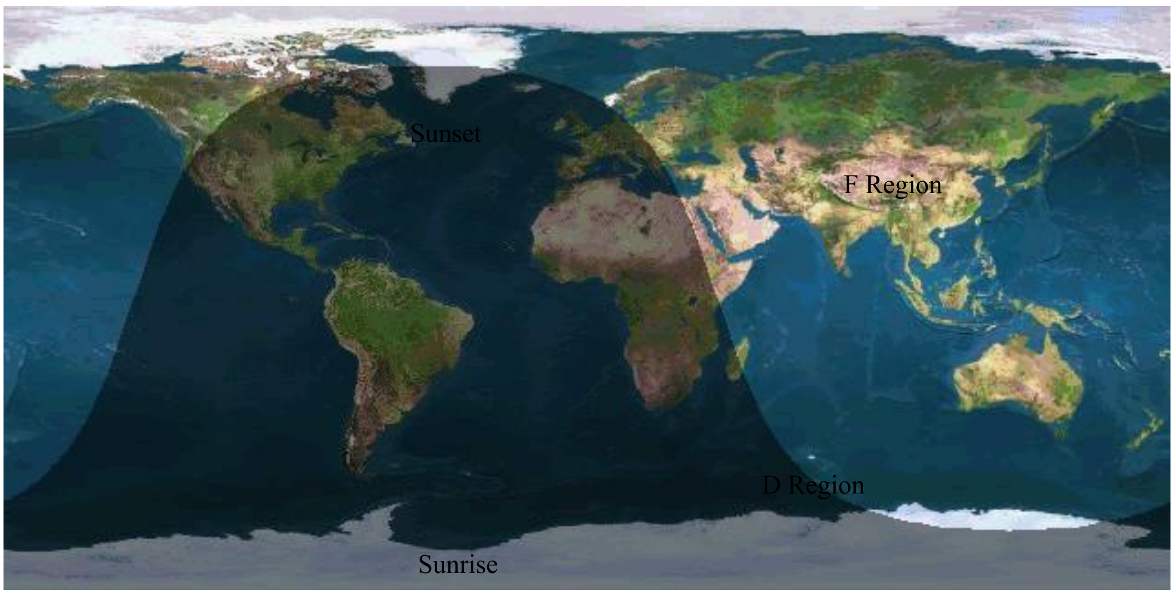

Figure 32 Gray line propagation

Since D level absorption is inversely proportional to frequency squared, gray line propagation is very important for 80 and 40 meter DX, less so for 20 meters, and usually not relevant for 18 through 10 meters.

$$Absorption \propto \frac{1}{f^2}$$

17.8 Equatorial Sporadic E Propagation

At low latitudes, ionization irregularities resulting from the equatorial electrojet are believed to be responsible for creating sporadic E patches. The patches appear daily in a band about 5º either side of the magnetic equator.

A low elevation angle signal can travel a considerable distance by reflecting from an equatorial sporadic E patch followed by a subsequent F layer refraction, as illustrated in Figure 33.

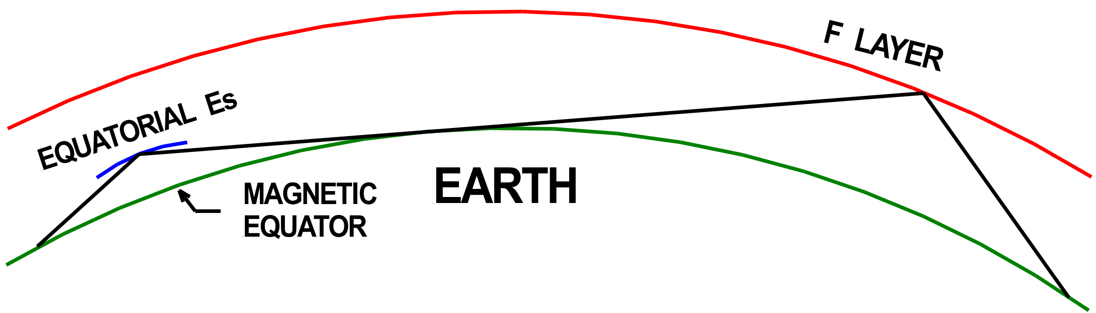

Figure 33 Equatorial Sporadic E propagation (source: author)

17.9 Transequatorial Propagation (TEP)

Transequatorial propagation is primarily a long distance 6 meter propagation mode between:

- Central America and South America,
- Japan and northern Australia,
- The Mediterranean and South Africa

as illustrated in Figure 34.

Transequatorial propagation is caused by the equatorial fountain effect illustrated in Figure 35. During the day ions and electrons drift upward in the ionosphere due to the force exerted by perpendicular electric and magnetic fields along the geomagnetic equator. The electric field gradually weakens and finally disappears at an altitude of around 800 km. With the electric field no longer present, charged particles (ions and electrons) travel under the influence of gravity and pressure gradients along magnetic field lines that curve back to Earth as illustrated in Figure 35. The charged particles combine with those already in the region creating a peak or crest in electron concentrations 15 to 20º north and south of the equator while a trough, or deficiency of electrons, develops over the equator.

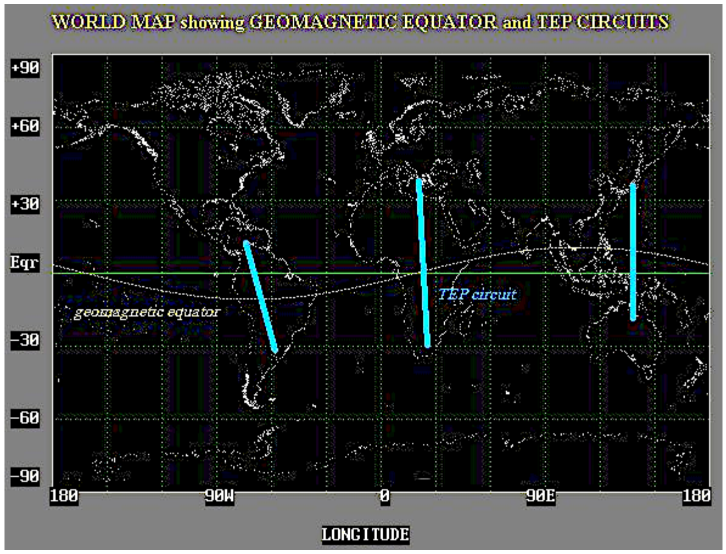

Figure 34 Transequatorial propagation paths (source: Australian Space Weather Services)

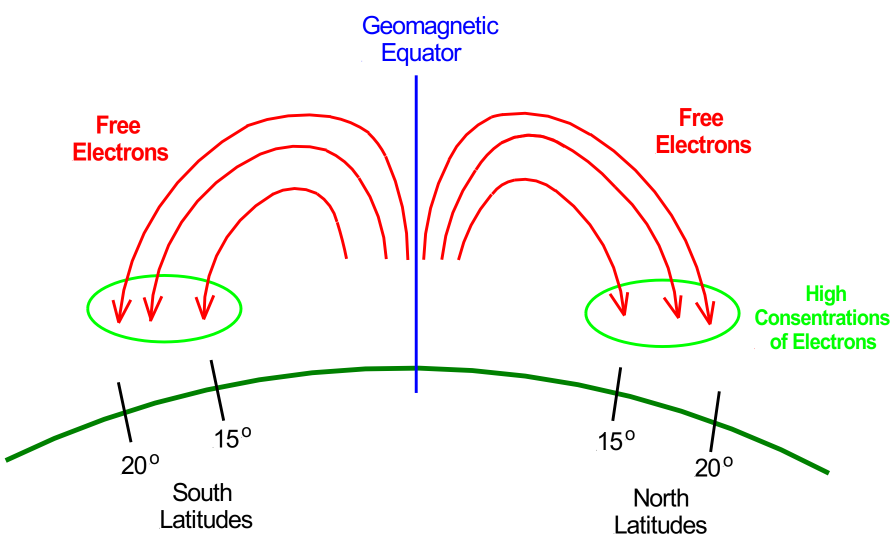

Figure 35 Equatorial plasma fountain (source: author)

Initially, before the fountain effect was understood, the high concentration of electrons appearing at latitudes between 15 to 20 degrees was known as the equatorial or Appleton anomaly. It was believed to be an anomaly since the highest electron concentrations were expected to occur over the equator.

The fountain effect is clearly visible in the winter (December) ionospheric map shown in Figure 36. The black line sloping through South America is the magnetic dip equator. The crests in electron concentrations are the bright pink zones on both sides of the magnetic equator.

The crests usually form in the late afternoon and early evening. While the crests vary from day-to-day and seasonally, they are most pronounced during solar maximum. Notice in Figure 36 that the largest electron peaks (two of them) occur in the winter hemisphere.

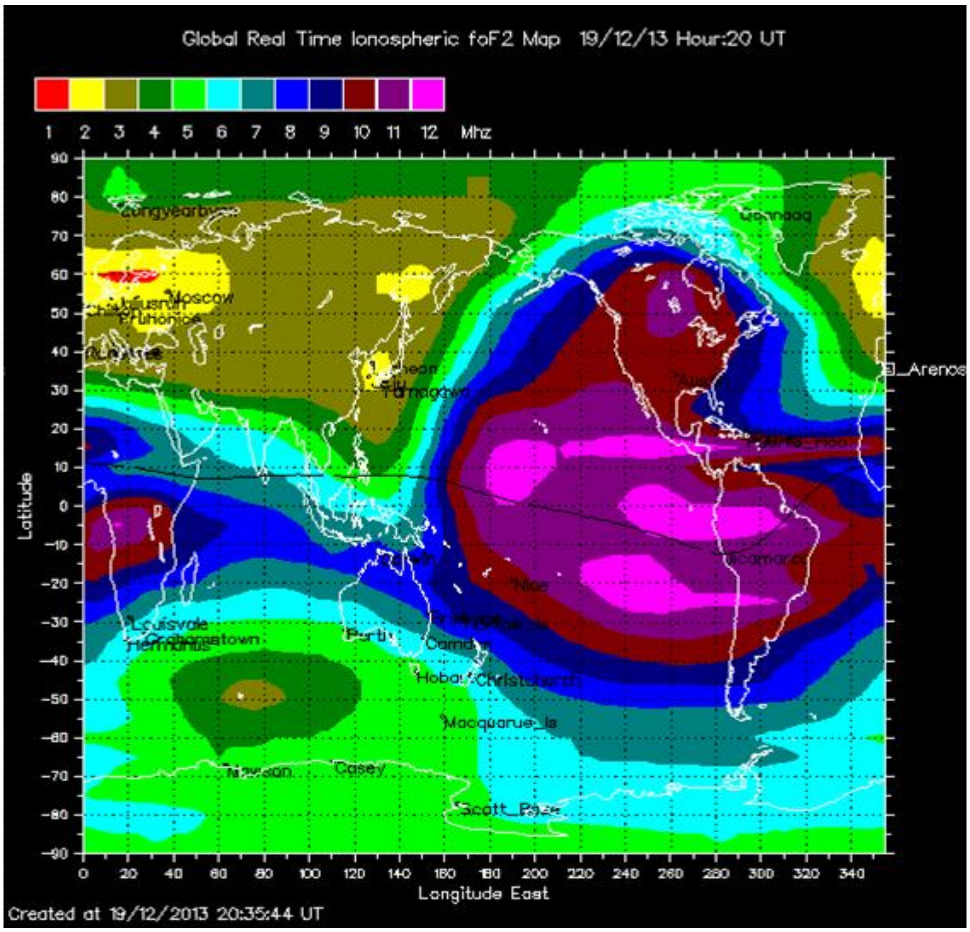

Figure 36 Ionospheric map showing fountain crests (source: Australian Space Weather Services)

F2 critical frequencies within the crests can often reach 18 MHz or higher during solar maximum. The maximum usable frequency at f_{cF2} = 18 MHz and an elevation angle E = 17^o is

$$[MUF]_{17^\circ} = \frac{f_{cF2}}{\sin E} = \frac{18\ MHz}{\sin 17} = 61\ MHz$$

The frequency of optimum transmission is

$$FOT = 0.85\ MUF = 0.85(61\ MHz) = 52.3\ MHz$$

occurring in the 6 meter frequency band. Because of the fountain effect and associated equatorial trough, critical frequencies along the magnetic equator are typically several MHz less than in the crests.

The fountain effect distorts the general form of the ionosphere throughout the low latitude equatorial region leading to the Transequatorial 6 meter propagation phenomena, as illustrated in Figure 37. Typically, a radio signal transmitted from one hemisphere to the other requires multiple hops through the ionosphere to reach its destination, with signal attenuations occurring with each hop. Instead, a radio signal experiencing Transequatorial propagation reflects off one fountain crest, travels across the equator to the second crest, and then reflects back to Earth. Transequatorial propagation allows a radio signal to traverse long distances from the transmitter to receiver in one hop, greatly minimizing signal loss.

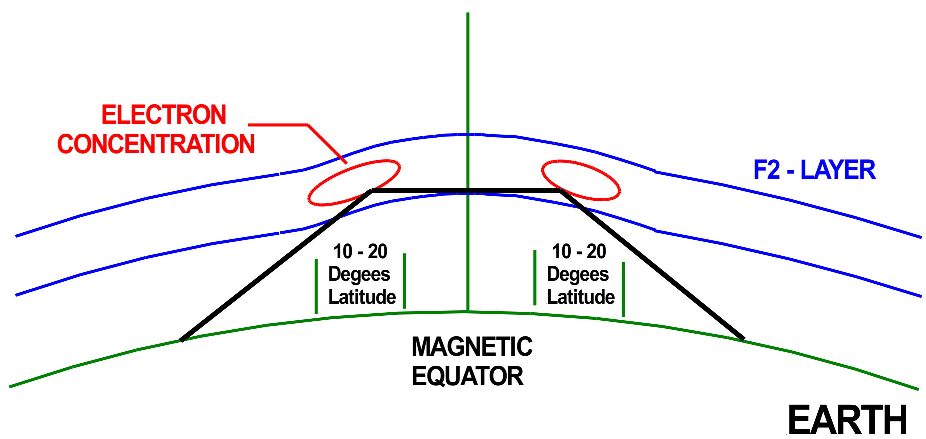

Figure 37 Transequatorial Propagation (source: author)

17.10 Ionospheric Ducting

If a signal is injected into the ionosphere at just the right angle, and under the right conditions, it can become trapped between the F and E layers, reflecting off the bottom of the F and the top of the E layer, as illustrated in Figure 38. This injection can sometimes occur when a signal reflects from ionospheric irregularities. A signal traveling in an ionospheric duct avoids multiple passes through the energy absorbing D layer and reflections from the ground. Consequently, the signal can travel a long distance with little signal loss. Experiencing ionospheric ducting is weird. When ducting is present, communications half way around the world can occur with the same signal strength, clarity, and stability as communicating locally on a 2 meter repeater.

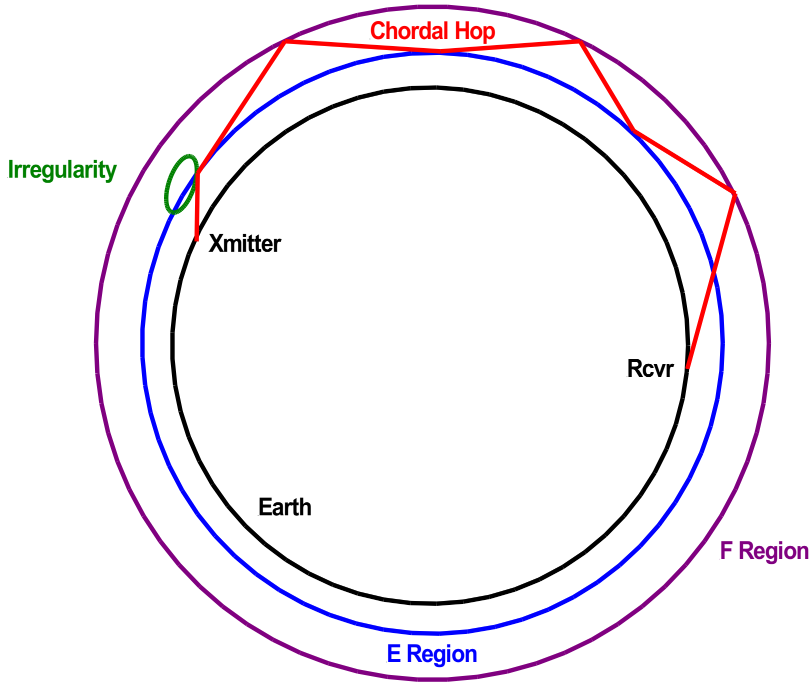

Figure 38 Ionospheric ducting (source: author)

References

Davies, Kenneth; “Ionospheric Radio”; Peter Peregrinus Ltd.,1990

McNamara, Leo F.; “The Ionosphere: Communications, Surveillance, and Direction Finding”; Krieger Publishing Company, 1991

Hunsucker R. D.; Hargreaves, J. K.; “The High-Latitude Ionosphere and its Effects on Radio Propagation”; Cambridge University Press 2003

Nichols, Eric P.; “Propagation and Radio Science”; The American Radio Relay League, Inc. 2015

Yeang, Chen-Pang; “Probing The Sky With Radio Waves”; The University of Chicago Press, 2013

Devoldere, John; “Low-Band DXing” fourth edition; ARRL, 2005

Levis, Curt A. ; Johnson, Joel T.; and Teixeira, Fernando L.; “Radiowave Propagation Physics and Applications”; John Wiley & Sons, Inc., 2010

Goodman, John M.; “Space Weather & Telecommunications”; Springer Science+Business Media Inc. 2005

Ahrens, C. Donald; “Essentials of Meteorology”; Wadsworth Publishing Company, 1998

UCAR Center for Science Education (UCAR SciEd); https://scied.ucar.edu/learning-zone/atmosphere/

Khazanov, George V.; “Space Weather Fundamentals”; CRC Press, 2016

Foukal, Peter; “Solar Astrophysics third edition”; Whiley-VCH Publishing Company, 2013

Ganushkina, N. Yu.; Liemohn, M. W.; Dubyagin. S.; “Current Systems in the Earth’s Magnetosphere”; AGU, March 8, 2018

Gallagher, Dr. D.L.; “The Earth’s Plasmasphere”; Space Plasma Physics, Marshall Space Flight Center, Huntsville, Al, September 05, 2018

Moore, T. E., Morwitz, J. L.; “Stellar Ablation of Planetary Atmospheres”; August 9, 2007

Yau, Andrew W.; Abe, Takumi; Peterson, W. K.; “The Polar Wind: recent Observations”; Department of Physics and Astronomy, University of Calgary

Carroll, Bradley W. and Ostlie, Dale A.; “An Introduction to Modern Astrophysics”; Addison-Wesley Publishing Company Inc., 1996

Cander, Ljiljana R.; “Ionospheric Space Weather”; Springer Nature Switzerland AG 2019

Moldwin, Mark; “An Introduction to Space Weather”; Cambridge University Press, 2008

Campbell, Wallace H.; “Introduction to Geomagnetic Fields”; Cambridge University Press, 2003

Golub, Leon and Pasachoff, Jay M.; “Nearest Star The Surprising Science of Our Sun second edition”; Cambridge University Press, 2014

Loff, Sarah: ”Explorer and Early Satellites”; National Aeronautics and Space Administration, Aug 3, 2017

Minzner, R. A.; “The 1976 Standard Atmosphere Above 86 km Altitude” NASA Goddard Space Flight Center, 1976